APL Energy

RESEARCH ARTICLE | JANUARY 25 2024

Transforming scalable synthesis of graphene aerosol gel material toward highly flexible and wide-temperature tolerant printed micro-supercapacitors

Kh M Asif Raihan ; Surjit Sahoo ; Thiba Nagaraja; Shusil Sigdel; Brice LaCroix; Christopher M. Sorensen ; Suprem R. Das

APL Energy 2, 016104 (2024)
https://doi.org/10.1063/5.0186302

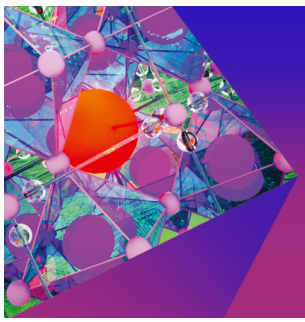

Transforming scalable synthesis of graphene aerosol gel material toward highly flexible and wide-temperature tolerant printed micro-supercapacitors

Cite as: APL Energy 2, 016104 (2024); doi: 10.1063/5.0186302
Submitted: 5 November 2023 • Accepted: 4 January 2024 •
Published Online: 25 January 2024

Kh M Asif Raihan,[1] Surjit Sahoo,[1] Thiba Nagaraja,[1] Shusil Sigdel,[2] Brice LaCroix,[3] Christopher M. Sorensen,[2] and Suprem R. Das[1,4,a)]

AFFILIATIONS

[1] Department of Industrial and Manufacturing Systems Engineering, Kansas State University, Manhattan, Kansas 66506, USA
[2] Department Physics, Kansas State University, Manhattan, Kansas 66506, USA
[3] Department of Geology, Kansas State University, Manhattan, Kansas 66506, USA
[4] Department of Electrical and Computer Engineering, Kansas State University, Manhattan, Kansas 66506, USA

[a)] **Author to whom correspondence should be addressed:** srdas@ksu.edu

ABSTRACT

The ever-growing demand for portable, bendable, twistable, and wearable microelectronics operating in a wide temperature range has stimulated an immense interest in the development of solid-state flexible energy storage devices using scalable fabrication technology. Herein, we developed additively manufactured graphene aerosol gel-based all-solid-state micro-supercapacitors (MSCs) via inkjet printing with functioning temperature in the range from −15 to +70 °C and exhibiting a super-stable and reliable electrochemical performance using interdigitated finger electrodes and PVA/H_3PO_4 solid-state electrolyte. The graphene aerosol gel was obtained using a scalable single step synthesis method from a gas phase precursor using a detonation process, producing a nanoscale shell type structure. The fabricated graphene aerosol gel-based solid-state MSC achieved a volumetric capacitance of 376.63 mF cm^{-3} (areal capacitance of 76.23 μF cm^{-2}) at a constant current of 0.25 μA and demonstrated exceptional cyclic stability (~99.6% of capacitance retention) over 10 000 cycles. To exploit the mechanical strength of the as-fabricated graphene aerosol gel-based solid-state MSC, its supercapacitive performance was scrutinized under various bending and twisting angles and the results showed excellent mechanical flexibility. Furthermore, to study the electrochemical performance of the as-fabricated graphene aerosol gel solid-state MSC in stringent surroundings, a broad temperature dependent supercapacitive analysis was performed as stated above. The electrochemical results of the as-fabricated graphene aerosol gel based all-solid-state MSC exhibit a highly potential route to develop scalable and authentic future miniaturized energy storage devices for IoT based smart electronic appliances.

I. INTRODUCTION

Embedding power sources into electronics is an ever-growing concern in microelectronics as the power source units do not scale proportionately as the CMOS chips. Moreover, high performance computing advances demand a new class of hybrid and sustainable power sources that are yet to be developed. Supercapacitors are devices known for their high performance deliverance and the need for a printed supercapacitor in all-solid-state form on ubiquitous substrates, including on flexible and bendable platforms; therefore, they have a great impact on a variety of electronics, including wearable electronics, wireless sensors, implantable medical devices, micro-robots, and microelectromechanical systems (MEMS).[1–3] Co-designing scale-down computing and power devices could further be exploited in complex IoT devices, including live monitoring of signal and feedback control in many of the modern

technological developments in the 21st century. Therefore, there is a great demand for lightweight flexible microbatteries and micro-supercapacitors (MSCs) as micropower (μ-power) units for powering smart electronic devices.[4,5] MSCs have been demonstrated as favorable micropower sources with fast charge–discharge rates, a high power density, and an ultralong cycle life.[6,7] Till now, most improvements in the electrochemical performance of MSCs have concentrated on proper selection of electrode materials with a high surface area to enhance the specific energy (both volumetric and areal) and a long cycle life combined with outstanding flexibility. Therefore, great effort has been made for the development of electroactive materials for the fabrication of MSCs.[8,9]

Amid all electroactive materials, graphene becomes a highly encouraging contender for high-performance flexible MSCs due to its large surface area, high theoretical capacitance, and exceptional intrinsic electrical and mechanical properties.[10–12] Numerous techniques have been established to fabricate MSCs based on graphene electrodes. In 2014, Wu *et al.* developed a photolithography technique to fabricate all-solid-state, planar interdigital graphene-based MSCs.[13] Later, this photolithography technique was commonly used for the fabrication of interdigitated patterns of MSCs. However, the photolithography technique suffers from its high cost and indispensable sacrificial templates for the fabrication of MSCs. Similarly, laser scribing and reduction technologies are matured compared to photolithography techniques for fabricating micro-sized graphene electrodes with high-resolution patterns. However, the laser scribing technique can only work for limited electroactive materials.[6] Printing supercapacitor devices possess a promising route for large scale manufacturing of energy storage devices.[14–16] Screen printing is widely used for scalable fabrication of MSCs; however, the process needs a mesh screen as a mask limits the customizability of the MSC design and the printing resolution. Therefore, to fabricate all-solid-state MSCs using nanoscale materials (such as graphene) in a scalable and sustainable manner at low cost and high resolution with a customizable design, inkjet printing technology has been widely utilized.[17,18] In recent years, a number of research studies have been conducted in developing sustainable large-scale production of graphene and their exploration in graphene-based inks for inkjet printing for myriad applications, including supercapacitors. However, further energy-efficient, affordable, and sustainable manufacturing routes to produce graphene and engineered graphene-based functional materials are necessary for affordable printable technologies.[19] For example, Li and co-workers demonstrated the scalable fabrication of graphene based MSCs on a silicon wafer and Kapton films with a good electrochemical performance.[20] Synthesizing a high-quality graphene-based ink with tunable rheology at a large scale for the fabrication of MSCs with high-performance metrics is still challenging.

Various promising additive manufacturing techniques with high resolution capabilities, such as inkjet printing, gravure printing, and aerosol jet printing, using graphene and graphene based materials as a matrix have shown promise due to the recent emphasis on the development of large scale graphene synthesis through low-cost liquid-phase processing.[21] However, high volume manufacturing of graphene aerosol gel materials with a tunable conductivity and surface interfacial properties and their use in manufacturing printable inks have not been emphasized. A gas phase detonation process exploiting a hydrocarbon fuel with a minimal oxygen mixture constitutes a novel approach for manufacturing graphene aerosol gel type materials. In our previous work, we have shown a graphene aerosol gel ink and its use in printed MSCs using ionic liquid electrolytes.[12] However, in this work, a further optimal material synthesis of a graphene aerosol gel has been made by varying hydrocarbon to oxygen ratios with an improved electrical conductivity and its use for all-solid-state MSCs fabrication is reported. Additionally, the development of robust MSCs having extreme mechanical flexibility with a wide temperature tolerant performance needs to be addressed.[22,23] The unique nanoscale structure of the graphene aerosol gel resembles a quasi-three-dimensional shell-like geometry that could provide a tortuous path for reinforcing the electrolyte in the printed structure and addressing any associated strain due to bending and twisting. The graphene aerosol gel ink was stable over months and easy to use in printing the interdigitated structured graphene aerosol gel electrodes with a high resolution for fully solid-state MSC fabrication without using any current collectors, a conductive additive, and separators. The fabricated graphene aerosol gel based solid-state MSC exhibits a volumetric capacitance of about 376.63 mF cm^{-3} (areal capacitance of 76.23 μF cm^{-2}) at an applied current of 0.25 μA with an excellent cyclic stability of 99.6% over 10 000 cycles. Additionally, we have studied the mechanical flexibility of the as fabricated graphene aerosol gel based solid-state MSCs and found negligible capacitance changes (after long cycles) at various bending states. Finally, we successfully demonstrated the temperature-dependent supercapacitive performance of graphene aerosol gel based solid-state MSCs through a wide range of temperatures (−15 to +70 °C). The electrochemical performance of industrially scalable graphene aerosol gel based solid-state MSCs offers a new avenue for facile, all-solid-state, and flexible energy storage devices for microelectronics applications.

II. EXPERIMENTAL METHOD

A. Graphene synthesis

The aerosol gel graphene was synthesized using a detonation based scalable one-step synthesis method described in previous studies.[23] In short, volumetric 70% acetylene and 30% oxygen were controllably detonated at a high temperature in a 17 L aluminum chamber. This high heat energy plays a critical role in the formation of the aerosol gel graphene yielding 7.5 g in each batch, which can be scaled up to the kilogram scale in each batch with a bigger detonation chamber.[23]

B. Ink formulation

The as-made aerosol gel graphene was first infused with ethyl cellulose, which acted as a binder to improve the solubility and flowability of the graphene ink. Ethyl cellulose was first dissolved in 50 ml of ethanol in 2 mg/ml concentration through ultrasonic bath sonication. Then, 250 mg of graphene powder was added to the solution and was subjected to a high sheer force using an ultrasonic probe sonicator (Qsonica 500, 20 KHz) to form a homogeneous dispersion. The dispersion was collected and filtered through a 5 μm filter to get rid of any remaining large agglomeration. Then, the filtered dispersion was flocculated with NaCl and filtered in a vacuum filtration system using a 47 mm diameter 0.45 μm cellulose filter (Sigma-Aldrich). The filtrate powder was

dried overnight in a hotplate at 50 °C and can be stored for a long time to make ink as required. Finally, the printable graphene ink was formulated by uniformly suspending the graphene/EC powder in a binary solvent system (cyclohexanone:terpineol = 85:15) with the help of ultrasonic bath sonication for 2 h. The prepared ink was tested stable over several months while stored at 9–11 °C in a refrigerator.

C. Electrode printing

To print the interdigitated supercapacitor, electrodes with high precision Microplotter II from SonoPlot Inc. were used, which was equipped with a piezoelectric 40 μm glass nozzle. The in-built drawing software was used to create the graphics and to define the dimensions of the interdigitated electrodes. The electrodes were printed on a 25 μm polyimide film (Sigma-Aldrich), which was thoroughly cleaned in an acetone, methanol, and IPA solvent using an ultrasonic cleaner. Once the printing was finished, the printed electrodes were annealed at 350 °C on top of a hot plate for 2 h to get rid of the organic no conductive binder.[12]

D. Electrolyte preparation

The PVA-H_3PO_4 electrolyte was prepared by dissolving 1 g of polyvinyl alcohol in 10 ml of deionized water at a high temperature under continuous and rigorous stirring. When the solution color became transparent and all the PVA was dissolved homogeneously in water, the solution was cooled down to room temperature. At room temperature, 0.8 g of concentrated H_3PO_4 (85 wt. % aqueous solution, Sigma-Aldrich) was added to the solution and magnetically stirred for 12 h to ensure the formation of a homogeneous mixture. The prepared electrolyte was stored in a vacuum chamber before printing the electrolyte, and it was always heated at 60 °C for 10 min to ensure a better contact at the interface so that no air can be entrapped in between them.

E. Silver paste printing

A Voltera V-one PCB printer was used to print conductive ink (silver paste) on the electrode contact point. The square pattern was drawn in the KiCad open resource software, and after sample set up and alignment, the conductive ink was mounted on the robotic arm of the printer, which can control the deposition of ink by mechanical gear mechanism. After printing the silver ink contact, the electrodes were heated at 200 °C for 10 min to get rid of any residual organic materials in the ink and to solidify the contact point.

F. Electrolyte printing

The electrolyte was also printed using the Voltera V-one printer. The prepared electrolyte was always heated at 60 °C for 10 min to ensure a better contact at the interface so that no air can be entrapped in between. Then, the electrolyte was loaded into the ink holder and mounted on the robotic arm. An 8×7 mm^2 rectangular pattern was drawn and printed to ensure that the electrolyte layer covers the whole device. After electrolyte printing, the device was air-dried for 24 h to complete the fabrication of the solid-state micro-supercapacitor.

III. RESULTS AND DISCUSSION

Figure 1(a) shows the schematic diagram of the formulation of graphene aerosol gel-based printable inks. An ultrasonication process is involved for the homogeneously suspended graphene aerosol gel-based ink as shown in the figure. The complete procedure involving the fabrication of an inkjet-printed graphene aerosol gel based all-solid-state MSC in an interdigitated electrode (IDE) configuration is shown in Fig. 1(b). The physical size realization of our graphene aerosol gel based solid-state MSC is made by placing a representative MSC on a human fingertip and tree leaf [Figs. 1(c) and 1(d)].[24] The uniformity and surface morphology of the printed pattern were investigated using a low- and high-resolution scanning electron microscope (SEM), as shown in Figs. 1(e)–1(g). The captured micrograph of the electrode fingers showed uniform printing features without any coffee ring effect. The measured dimensions were as per the design features made using the CAD software of the inkjet printer (Sonoplot Microplotter). The high-resolution SEM taken on the IDE fingers reveals an abundance of nanoscale shell-like structures which can impart increasing porosity in the electrodes so that the electrolyte can have a better interaction with the electrode material, which positively influences the capacitance. The Raman spectra of the as-prepared graphene aerosol gel ink and associated materials are provided in Fig. S1 and discussed in detail (see the supplementary material). Furthermore, high resolution transmission electron microscopy (TEM) was performed on the graphene aerosol gel ink material to further analyze the crystal structure and the number of graphene layers [shown in Figs. 1(h) and S2]. The TEM micrographs reveal a multi-layered, crumpled, and shell-like structure of the graphene aerosol gel, which is in agreement with a previous report.[12] Multiple walls seen and counted in a single graphene shell structure in the TEM are in agreement with the broad FWHM and lower intensity of the 2D peak in the Raman spectra. The Raman spectra also provide the signature of an intense D peak in this graphene aerosol gel ink material. The origin and significance of these fundamental graphene characteristics, including the defects, on the energy storage characteristics is yet to be fully understood in our future work. To understand the average shell heights/thicknesses, atomic force microscopy (AFM) was used, and the result is shown in Fig. 1(i) in the range of 4.5–6.5 nm, indicating non-spheroid graphene shell platelets. As these structures are not flat sheets of graphene, it is challenging to directly interpret the exact number of atomic layers from the AFM thickness measurements, although correlating the Raman spectra and TEM analysis, it can be proposed that there are 5–10 layers of graphene sheets forming the walls of the shell-like graphene aerosol gel particles. To obtain the elemental distributions of the as-prepared graphene aerosol gel ink material, energy dispersive x-ray spectroscopy (EDS) analysis was performed, and the result is shown in Fig. S3, indicating the presence of carbon and oxygen.

To demonstrate the energy storage performance of the inkjet-printed graphene aerosol gel IDE and PVA-H_3PO_4 gel as the solid-state electrolyte based MSCs, a series of electrochemical tests were carried out in a two-electrode configuration to estimate the supercapacitive performance of in-plane, mechanically flexible, wide-temperature tolerant, and all-solid-state MSCs. To understand the dimension of our graphene aerosol gel based solid-state MSC, the schematic diagram and the tabulated dimensional parameters are

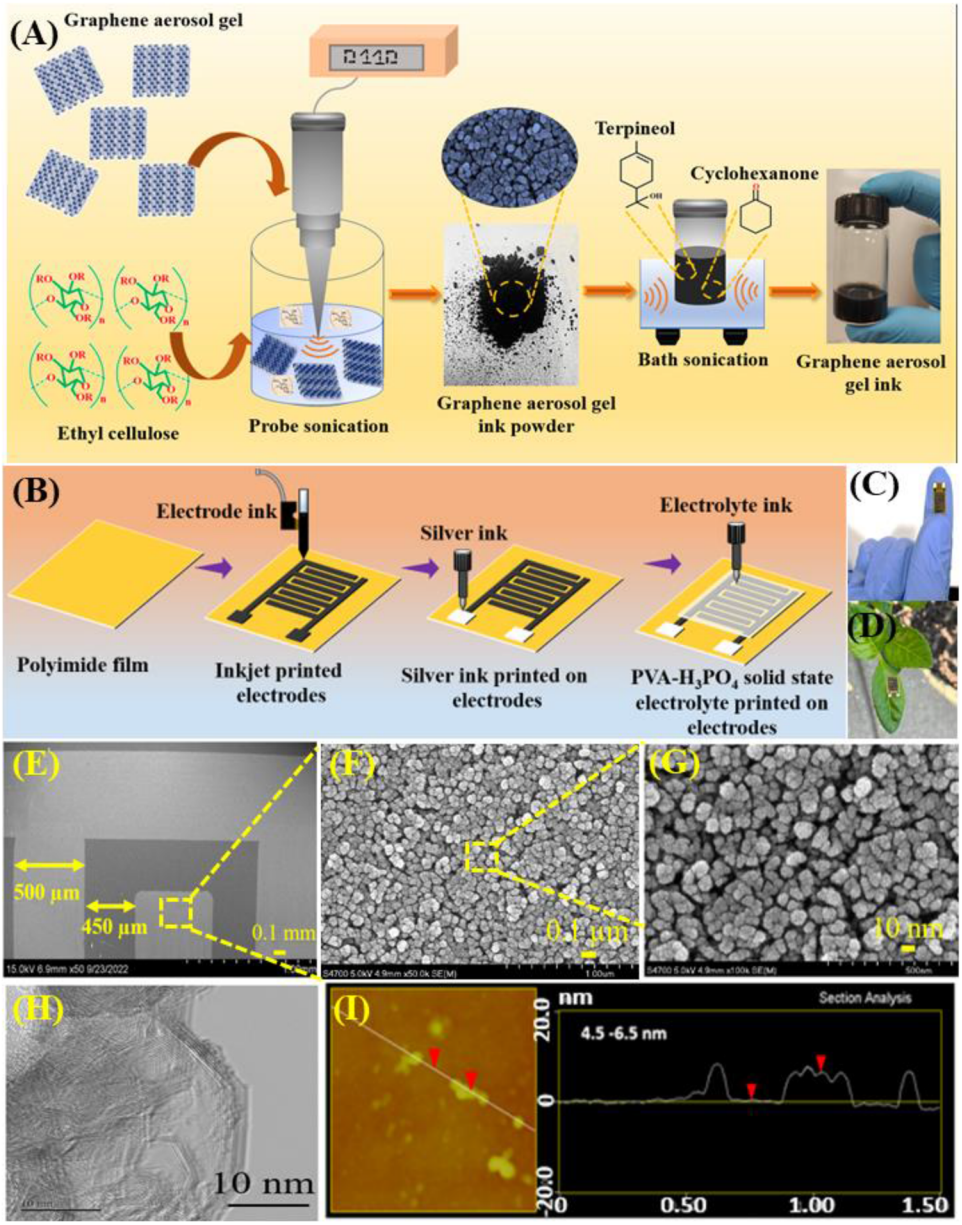

FIG. 1. (a) Schematic diagram of the graphene aerosol gel, binder/surfactant addition with the solvent and the graphene aerosol gel-based ink formulation. (b) Schematic illustration of the detailed fabrication process of the graphene aerosol gel based all-solid-state MSC using inkjet printing technology. (c) Graphene aerosol gel based all-solid-state MSC on fingertip. (d) Floating of the graphene aerosol gel based all-solid-state MSC on the tree leaves. (e)–(g) SEM micrographs of inkjet printed graphene aerosol gel based interdigital microelectrodes with various magnifications. (h) TEM micrograph of the graphene aerosol gel ink. (i) Atomic force microscopy images of the graphene aerosol gel ink.

provided in Figs. S4(a) and S4(b). Similarly, the SEM cross-sectional micrograph of the inkjet-printed graphene aerosol gel on the polyimide film is provided in Fig. S4(c), which indicates that the average thickness of graphene aerosol gel material on polyimide film is about ~2 μm. The real-time image of the as-fabricated graphene aerosol gel based solid-state MSC is shown in Fig. S5(a).

Figures 2(a) and 2(b) display the cyclic voltammetry (CV) profiles of graphene aerosol gel based solid-state MSC recorded over 1.0 V with various applied sweep rates (from 5 to 500 mV s^{-1}). The CV profile of the graphene aerosol gel based solid-state MSC is rectangular in nature at a very low sweep rate (5 mV s^{-1}), and it holds the nature even with an increase in the sweep rate of

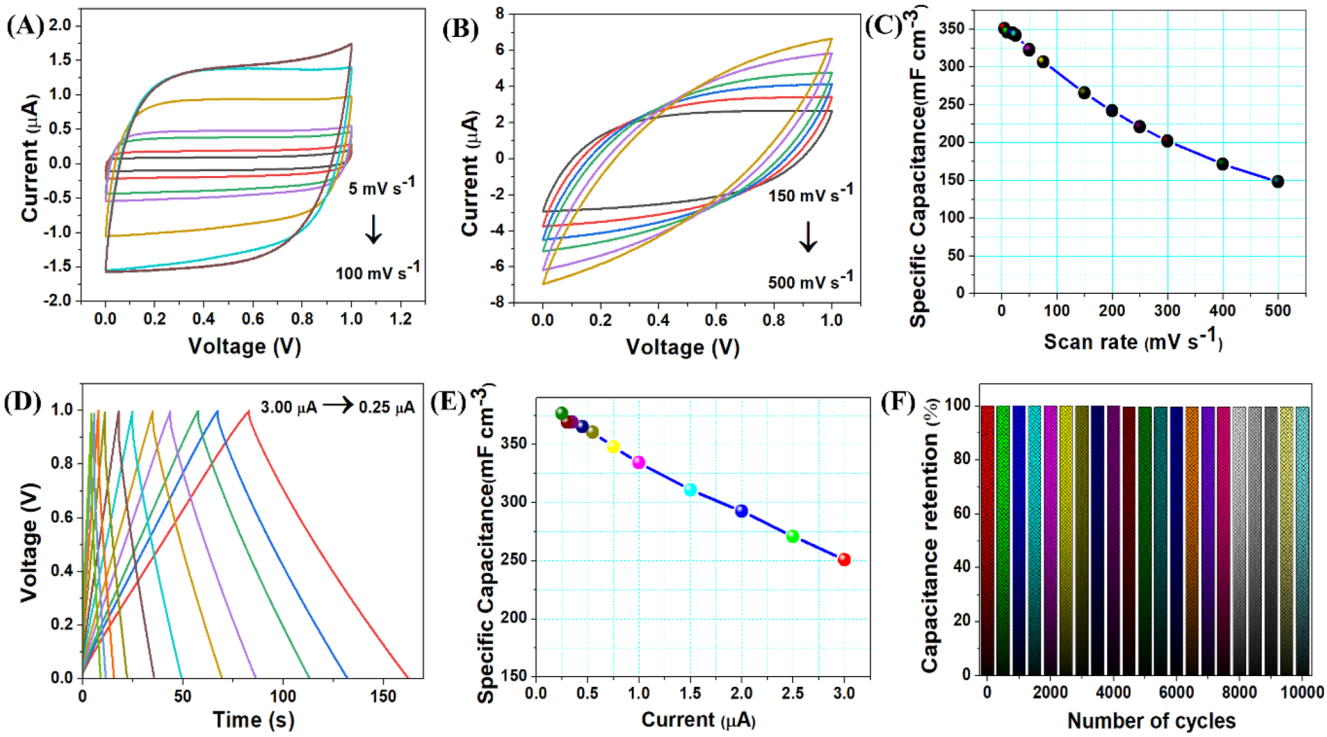

FIG. 2. Electrochemical characterization of the graphene aerosol gel based all-solid-state MSC using PVA/H_3PO_4 gel as the solid-state electrolyte. CV profile of graphene aerosol gel based solid-state MSCs at various scan rates: (a) from 5 to 100 mV s^{-1} and (b) 150–500 mV s^{-1}. (c) The plot of volumetric capacitance with respect to scan rates. (d) CD profile of graphene aerosol gel based solid-state MSCs at various applied currents. (e) The plot of volumetric capacitance with respect to the applied currents. (f) Long cyclic stability test of the graphene aerosol gel based solid-state MSC over 10 000 cycles.

100 mV s^{-1} (20-fold), signifying a better capacitive behavior of graphene aerosol gel based solid-state MSCs.[25] However, the shape of CV profiles [in Fig. 2(b)] changes from rectangular to quasi-rectangular nature with an increase in the sweep rates (>150 mV s^{-1}), which can be explained by the internal resistance and limited mass transport of electrolyte ions at the higher sweep rates.[26] The effect of sweep rates on the volumetric capacitance of graphene aerosol gel based solid-state MSCs is provided in Fig. 2(c), indicating that a high volumetric capacitance of 351.05 mF cm^{-3} was obtained at a low sweep rate of 5 mV s^{-1}. The graphene aerosol gel based solid-state MSC maintains about 42.20% of its initial volumetric capacitance, even when the sweep rate is increased 100-fold (500 mV s^{-1}), suggesting a better rate performance of the graphene aerosol gel based solid-state MSC.[27] The galvanostatic charge–discharge (CD) profile of the graphene aerosol gel based solid-state MSC at various applied currents (from 3 to 0.25 μA) is provided in Fig. 2(d), which indicates the symmetric triangular shape of the CD profile, and based on the applied current, the behavior of charge–discharge profiles become rapid at high current ranges and vice versa. The five continuous CD profiles of the graphene aerosol gel based solid-state MSC are recorded at a constant applied current of 1 μA, as shown in Fig. S5(b), indicating a triangular shape of CD with a good symmetry in the successive cycles.[28] Interestingly, the graphene aerosol gel based solid-state MSC obtains a coulombic efficiency of about ~98% at various charge–discharge cycles. The effect of the applied current ranges on the volumetric capacitance of the graphene aerosol gel based solid-state MSC is provided in Fig. 2(e). The MSC demonstrated the highest volumetric capacitance of 376.63 mF cm^{-3} at the lowest applied current of 0.25 μA. Similarly, the effect of the sweep rate on areal capacitance and the effect of the applied current on areal capacitance of the graphene aerosol gel based solid-state MSC are shown in Figs. S6(a) and S6(b). The fabricated MSC obtained a highest areal capacitance of 71.05 μF cm^{-2} at a sweep rate of 5 mV s^{-1} (from CV profile) and 76.23 μF cm^{-2} at an applied current of 0.25 μA (from CD profile). The volumetric Ragone plot and the areal Ragone plot for the graphene aerosol gel based solid-state MSC are provided in Fig. S7(a). The graphene aerosol gel based solid-state MSC delivers a volumetric energy density value of 52.3 μWh cm^{-3} at the volumetric power density of 2.38 mW cm^{-3} and it was able to retain 34.8 μWh cm^{-3} when the graphene aerosol gel based solid-state MSC obtained a higher power density of 28.5 mW cm^{-3}. In order to carry out the long-term cyclic stability of the as-prepared graphene aerosol gel based solid-state MSC, a continuous CD test was performed at a constant applied current of 1 μA over 10 000 cycles as shown in Fig. 2(f). The graphene aerosol gel based solid-state MSC exhibits excellent capacitance retention (~99.6%) over 10 000 cycles. Figure S7(b) represents the CD profile of the graphene

aerosol gel based solid-state MSC at the initial cycle and at 10 000 cycles, portraying the initial cycle charge–discharge profile and the final cycle charge–discharge as almost identical. The achieved capacitance retention (99.6%) over 10 000 cycles of the graphene aerosol gel based solid-state MSC is higher compared to the recently reported solid state MSC, such as, cellular graphene (97.6%),[25] porous carbon (94%),[29] LSG/SWCNTs (88.6%),[30] graphene–carbon sphere (95%),[31] reduced graphene oxide (94.6%),[32] laser-scribed graphene (87%),[33] and graphene (99%).[34]

Micro-energy storage systems with a customized voltage and current output by modular connections (series and/or parallel) are highly required to meet the real-time applications, and the printing/additive manufacturing method is a very attractive technique to realize the development of such modular energy storage systems.[35] Graphene aerosol gel based solid-state MSCs are assembled in series and/or parallel configurations [according to Figs. 3(a) and 3(d)] in order to achieve a tunable operating voltage and current output. Figure 3(b) represents the CV profile of graphene aerosol gel based solid-state MSCs in series connection (three devices), revealing an approximately rectangular shape of the graphene aerosol gel based solid-state MSC. The increase in working voltage from 1.0 to 3.0 V with the rectangular shape indicates the characteristic of EDLC. Similarly, the CD profile of the graphene aerosol gel based solid-state MSC (in series connection) was tested at an applied current of 1 μA and is shown in Fig. 3(c). The nature of CD profiles represents the proportional increase in the device voltage from 1.0 to 3.0 V when series connected from a single device to three devices, respectively. To confirm the electrochemical performance of the series connected devices (three devices), CV and CD tests were performed at various sweep rates (25–250 mV s^{-1}) and applied currents (3–0.2 μA), and the results are provided in Figs. S8(a) and S8(b). Furthermore, the electrochemical performance of parallelly connected graphene aerosol gel based solid-state MSCs was carried out using CV [Fig. 3(e)] and CD [Fig. 3(f)] tests. The CV profile indicates a rectangular shape with a proportionally increased area and/or current by combining the number of parallel MSCs from 1 to 3. Correspondingly, the discharge time of three parallel connected MSCs increases at the same applied current compared to a single MSC. The detailed CV and CD tests were performed for parallelly connected graphene aerosol gel based solid-state three MSCs and are shown in Figs. S9(a) and S9(b). This proof-of-concept demonstration of series and parallel graphene aerosol gel based solid-state MSCs can thus be accordingly additively

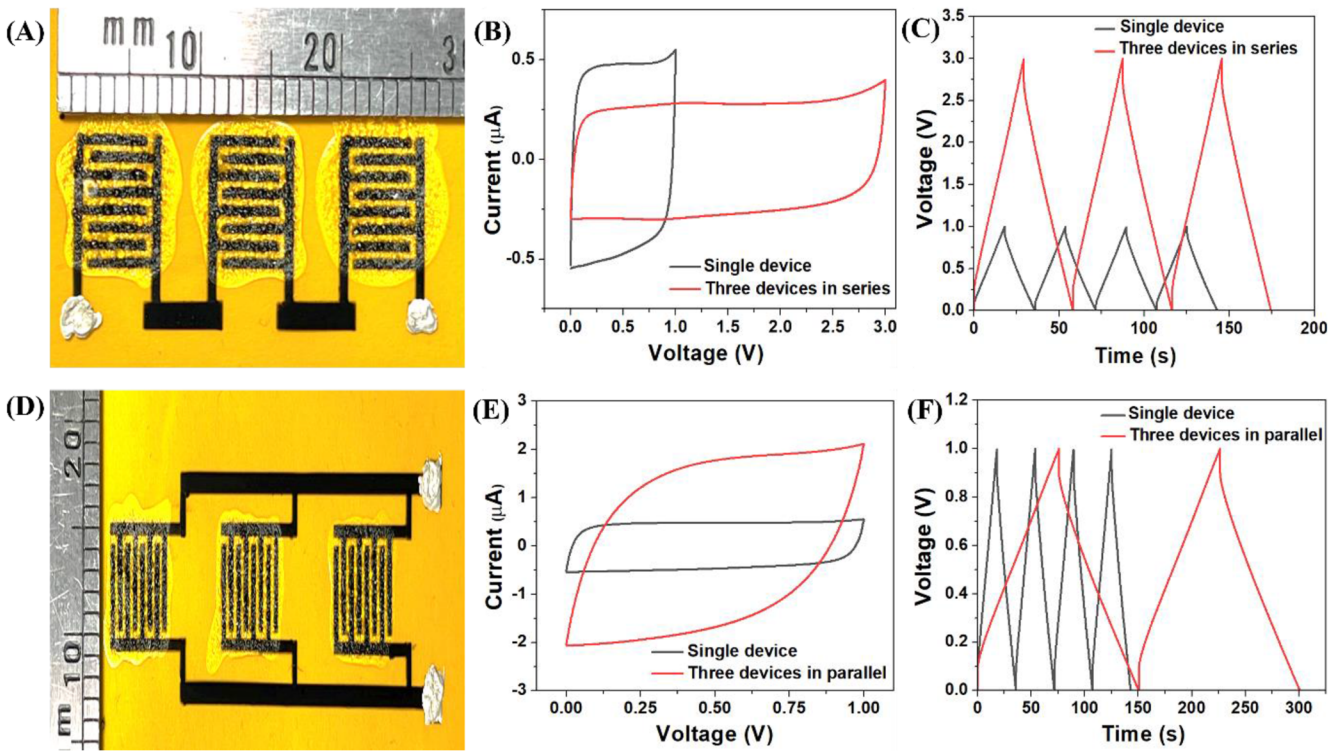

FIG. 3. (a) Digital image of the as-fabricated graphene aerosol gel based solid-state MSC connected in series. (b) CV profile of single and three graphene aerosol gel based solid-state MSCs connected in series at a scan rate of 100 mV s^{-1}. (c) CD profile of single and three graphene aerosol gel based solid-state MSCs connected in series at an applied current of 1 μA. (d) Digital image of the as-fabricated graphene aerosol gel based solid-state MSC connected in parallel. (e) CV profile of single and three graphene aerosol gel based solid-state MSCs connected in parallel at a scan rate of 50 mV s^{-1}. (f) CD profile of single and three graphene aerosol gel based solid-state MSCs connected in parallel at an applied current of 1 μA.

manufactured to achieve the desired working voltage in real-world electronic appliances.[36]

To establish the robust mechanical flexibility of the graphene aerosol gel based solid-state MSC, a series of electrochemical tests were carried out under various bending and twisting states. The comparative CV and CD profiles of graphene aerosol gel based solid-state MSCs at a constant sweep rate of 100 mV s^{-1} and a constant applied current of 1 μA under various bending states and are provided in Figs. 4(a) and 4(b), respectively. Remarkably, the CV and CD curves of graphene aerosol gel based solid-state MSCs are identical at various bending states. Figures 4(c)–4(e) and S10(a) represent the capacitance retention (over continuous 500 cycles) of graphene aerosol gel based solid-state MSCs under various bending states (radius of curvature ~7.5, 10, 15 and 4 mm). The graphene aerosol gel based solid-state MSC results in capacitance retention of 100%, 97.24%, 83.33%, and 80.33% under bending radius of 7.5, 10, 4, and 15 mm, respectively. A representative digital image of the graphene aerosol gel based solid-state MSC under bending condition (during electrochemical measurement) is shown in Fig. S10(b). Based on the various bending radii, corresponding bending angles for 500 charge–discharge cycles are shown in Fig. S11. The relatively less capacitive retention in the case of 15 mm bending radius (corresponding to 20° bending angle) could arise from a poor interfacial response between the graphene–polymer interface. Moreover, the graphene aerosol gel based solid-state MSC was fully twisted, and an electrochemical test was carried out over 500 cycles, as shown in Fig. 4(f). The twisted graphene aerosol gel based solid-state MSC exhibits capacitance retention of about 86.20% of the initial capacitance. These results indicate the excellent mechanical flexibility of the graphene aerosol gel based solid-state MSC, which is effective for powering next-generation wearable and portable devices.[37] These superior performances in bending and twisting are consistent with the characteristics of the nanoscale quasi-three dimensional shell-like structure of the constituent graphene aerosol gels discussed earlier.

In order to demonstrate the functionalities of the printed all-solid-state MSCs in harsher environments, such as cold and hot weather conditions, the electrochemical performance of the fabricated graphene aerosol gel based solid-state MSC was studied from −15 to 70 °C.[38,39] The digital image of the experimental setup for temperature-dependent supercapacitive analysis is shown in Fig. S12. Initially, the CV test was carried out at a constant sweep rate of 100 mV s^{-1} at various operating temperatures and is shown in Fig. 5(a). The shape of the CV profile maintains a quasirectangular shape at various operating temperatures, and the response (current values from the CV profile) of the graphene aerosol gel based

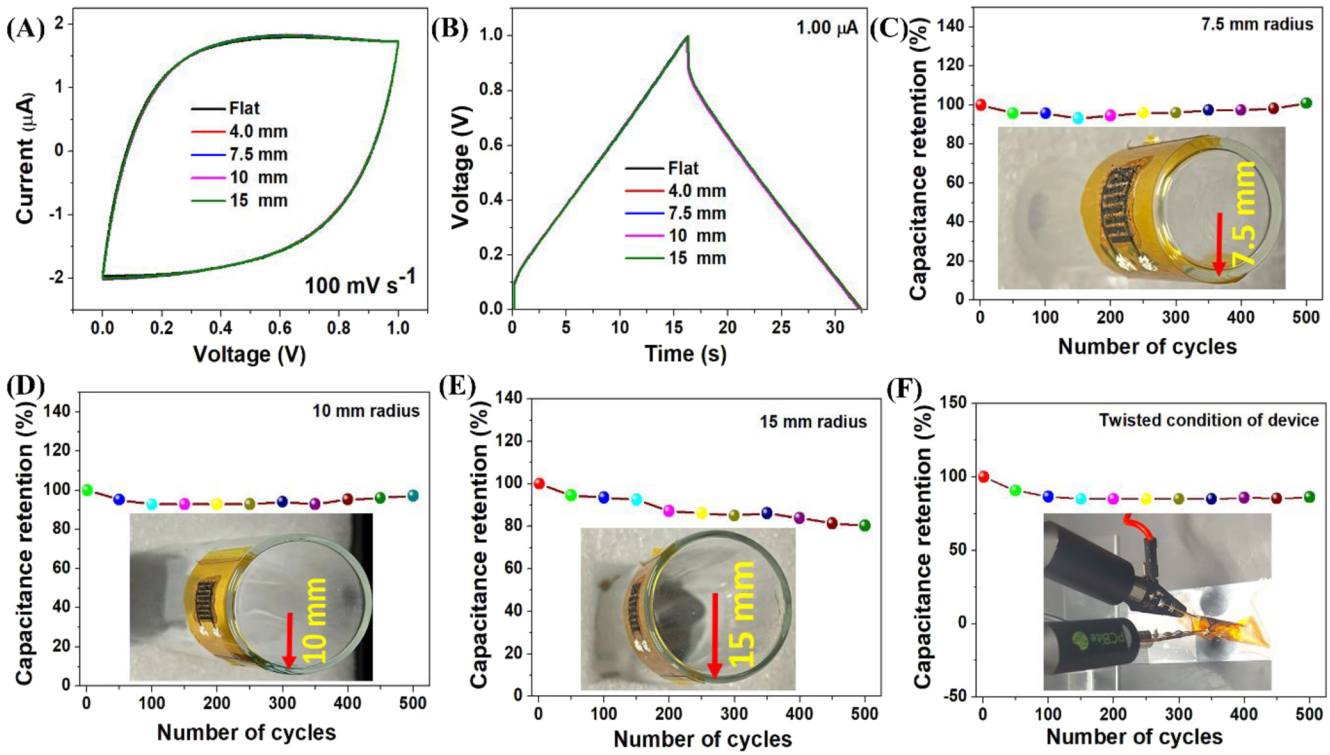

FIG. 4. Flexibility testing of the as-fabricated graphene aerosol gel based all-solid-state MSC. (a) CV profile of the graphene aerosol gel based solid-state MSC at various bending states (at a constant scan rate of 100 mV s^{-1}). (b) CD profile of graphene aerosol gel based solid-state MSCs at various bending states (at a constant applied current of 1 μA). Capacitance retention of graphene aerosol gel based solid-state MSCs over 500 cycles (c) at a bending state of 7.5 mm radius, (d) at a bending state of 10 mm radius, (e) at a bending state of 15 mm radius, and (f) under a fully twisted condition.

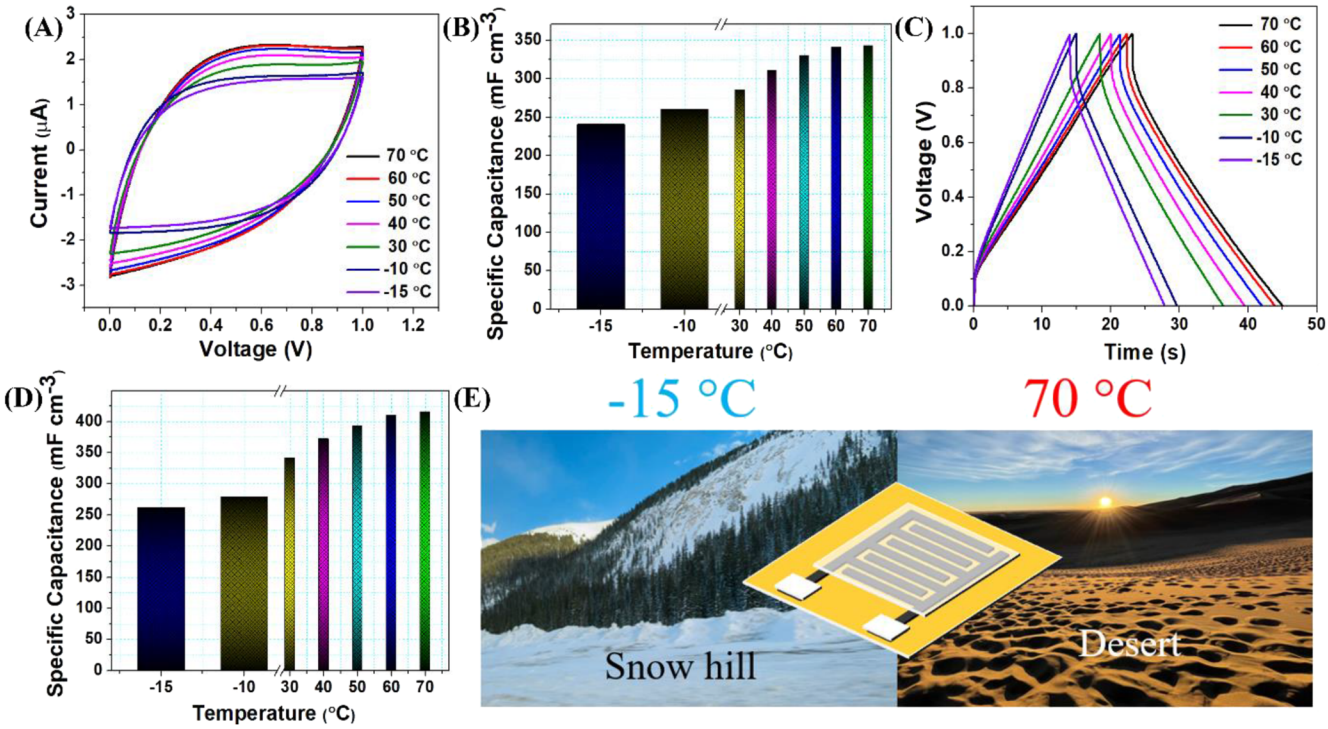

FIG. 5. Electrochemical investigation of graphene aerosol gel based all-solid-state MSCs at various levels of temperature in a solid-state electrolyte (PVA/H_3PO_4 gel). (a) CV profile of graphene aerosol gel based solid-state MSCs at various applied temperatures (from −15 to 70 °C). (b) The plot of volumetric capacitance (from CV profile) with respect to the applied temperature. (c) CD profile of graphene aerosol gel based solid-state MSCs at various applied temperatures (from −15 to 70 °C). (d) The plot of volumetric capacitance (from CD profile) with respect to the applied temperature. (e) Schematic illustration of the real time application of graphene aerosol gel based solid-state MSCs.

solid-state MSC displays linear enhancement in current when the operating temperature is increased from −15 to 70 °C, indicating an increase in the capacitance with an increase in operating temperature. The effect of the operating temperature on the volumetric capacitance of graphene aerosol gel based solid-state MSCs is shown in Fig. 5(b). The graphene aerosol gel based solid-state MSC exhibits a maximum capacitance of 343.37 mF cm^{-3} at an applied temperature of 70 °C and a minimum capacitance of 240.70 mF cm^{-3} at an applied temperature of −15 °C. To further clarify this behavior, the CD test was performed at the same temperature (from −15 to 70 °C) as CV. The CD test was carried out at a constant applied current of 1 μA and is shown in Fig. 5(c), which demonstrates an increase in charging and discharging time with an increase in the operated temperature (similar observation as in CV). The variation of volumetric capacitance with respect to various operating temperatures, as shown in Fig. 5(d), provides the maximum capacitance of up to 416.15 mF cm^{-3} at 70 °C from 262.21 mF cm^{-3} at −15 °C. The increase in capacitance by 158% at a higher temperature (70 °C) compared to the lower temperature (−15 °C) is due to the enhanced diffusivity and mobility of the electrolyte ions at a higher temperature. An increase in the operating temperature facilitates a reduction in the viscosity of the polymer electrolyte, resulting in a reduction in the interfacial resistance between electrode–electrolyte interfaces, higher ionic mobility, and forming intimate contacts between electrolyte and pore walls in the graphene aerosol gel structure. Consequently, the rate of diffusion of electrolyte ions can be accelerated with this low viscosity, which causes an increase in the overall conductivity of the electrolyte, and finally, this phenomenon results in the enhancement of electrochemical performances.[39,40] A similar trend also follows in the areal capacitance calculation, as shown in the Figs. S13(a) and S13(b). Fig. 5(e) illustrates a potential practical application of the studied MSCs in different climatic conditions (snowy place vs a hot desert). Since the technique used to manufacture their energy storage systems is adopted by an additive manufacturing scheme, MSCs of various shapes and sizes could be conceptualized and designed, as shown in in Figs. (S14)–(S16). The detailed electrochemical characterization (CV at various sweep rates and CD at various applied currents) are also shown in in Figs. (S14)–(S16). Interestingly, all these versatile-shaped MSCs displayed an almost expected CV and CD characteristics. The comparative performance table for various graphene based all-solid-state printed MSCs is provided in Table I. Table I indicates that our present work obtained a better capacitance (in both areal and volumetric) compared with that reported in the literature. The outstanding design flexibilities of the energy storage systems enabled by additive manufacturing, therefore, could be exploited to envision wide variety of applications, such as shape conformable wearable devices and IoT electronics for sensors.

TABLE I. Summary of electrochemical performances of graphene aerosol gel based solid-state micro-supercapacitors and recently reported micro-supercapacitors.

Sl no.	Electroactive material	Synthesis and fabrication	Electrolyte	Capacitance (volumetric and areal)	References
1	Reduced graphene oxide	Modified Hummers' method and mask deposition	PVA–H_3PO_4	19 μF cm^{-2}	41
2	$NiFe_2O_4$ nanofiber	Electrospinning and photolithography	PVA–KOH gel	67 μF cm^{-2}	42
3	Reduced graphene oxide	Modified Hummers' method and mask-free AxiDraw sketching	PVA/H_3PO_4	31.9 μF cm^{-2}	43
4	Activated carbon	Lithographically patterned	H_2SO_4	27 μF cm^{-2}	44
5	EDLC	Physical vapor deposition	LiPON	50 μF cm^{-2}	45
6	HF-etched Ti_3C_2	Hf etching and laser machining	PVA/H_2SO_4 gel	330 mF cm^{-3}	46
7	Graphene aerosol gel	Detonation synthesis and inkjet printing	PVA/H_3PO_4 solid-state	76.23 μF cm^{-2} (376.63 mF cm^{-3})	This work

IV. CONCLUSIONS

In summary, a wide-temperature tolerant all-solid-state and inkjet-printed micro-supercapacitor has been demonstrated using inks derived from graphene aerosol gel-based materials synthesized in the kilogram scale. The proof-of-concept method explored here could be further adopted for a scalable manufacturing of graphene aerosol gel based solid-state MSCs with robust mechanical flexibility for a number of potential applications, such as wearable and IoT electronics. The fabricated micro-supercapacitors exhibit highly reliable electrochemical performances, as revealed by a volumetric capacitance of 376.63 mF cm^{-3} (areal capacitance of 76.23 μF cm^{-2}) with excellent cyclic stability (~99.6% of capacitance retention) over 10 000 cycles, good integration ability, and robust mechanical flexibility. The highly stable and reliable results of these all-solid-state MSCs were attributed to the nanoscale shell-like structures of the graphene aerosol gels. Furthermore, results with high reliability, obtained from as low as −15 °C to as high as +70 °C temperatures, provide numerous opportunities for the scalable design of miniaturized energy storage devices for the next generation of microelectronics and microelectromechanical systems used in miniaturized Internet of thing technologies.

SUPPLEMENTARY MATERIAL

The supplementary material provides the electrochemical calculations, detailed Raman spectra characterization, TEM micrograph, EDS spectrum with mapping, additional CV and CD profiles, digital images and cyclic stability at various bending angles, and temperature dependent electrochemical performance of graphene aerosol gel based all-solid-state MSCs.

ACKNOWLEDGMENTS

S.R.D. acknowledges the support from HydroGraph Clean Power, Inc., and the U.S. National Science Foundation (NSF) Grant No. NSF CBET No. 1935676, for conducting this research. S.R.D. also acknowledges Jeffrey and Joy Lessman and Carl and Mary Ice Keystone Research scholarship for partial support of this work. S.S. acknowledges the funding from USIEF Award No. 2823 FNPDR/2022.

AUTHOR DECLARATIONS

Conflict of Interest

The authors have no conflicts to disclose.

Author Contributions

K.M.A.R. and S.S. contributed equally to this paper.

Kh M. Asif Raihan: Formal analysis (equal); Investigation (equal); Methodology (equal). **Surjit Sahoo**: Conceptualization (equal); Investigation (equal); Methodology (equal); Writing – original draft (equal); Writing – review & editing (equal). **Thiba Nagaraja**: Software (equal). **Shusil Sigdel**: Software (equal). **Brice LaCroix**: Resources (equal). **Christopher M. Sorensen**: Resources (equal). **Suprem R. Das**: Funding acquisition (equal); Project administration (equal); Supervision (equal).

DATA AVAILABILITY

The data that support the findings of this study are available within the article and its supplementary information.

REFERENCES

[1] L. Yu, Z. Fan, Y. Shao, Z. Tian, J. Sun, and Z. Liu, "Versatile N-doped MXene ink for printed electrochemical energy storage application," Adv. Energy Mater. **9**(34), 1901839 (2019).

[2] Aaryashree, S. Sahoo, P. S. Walke, S. K. Nayak, C. S. Rout, and D. J. Late, "Recent developments in self-powered smart chemical sensors for wearable electronics," Nano Res. **14**, 3669–3689 (2021).

[3] S. Sahoo, S. Ratha, C. S. Rout, and S. K. Nayak, "Self-charging supercapacitors for smart electronic devices: A concise review on the recent trends and future sustainability," J. Mater. Sci. **57**, 4399–4440 (2022).

[4] Z. Zhu, R. Kan, S. Hu, L. He, X. Hong, H. Tang, and W. Luo, "Recent advances in high-performance microbatteries: Construction, application, and perspective," Small **16**(39), 2003251 (2020).

[5] Q. Jiang, N. Kurra, C. Xia, and H. N. Alshareef, "Hybrid microsupercapacitors with vertically scaled 3D current collectors fabricated using a simple cut-and-transfer strategy," Adv. Energy Mater. **7**(1), 1601257 (2017).

[6] J. Wang, F. Li, F. Zhu, and O. G. Schmidt, "Recent progress in micro-supercapacitor design, integration, and functionalization," Small Methods **3**(8), 1800367 (2019).

[7] P. Zhang, J. Wang, W. Sheng, F. Wang, J. Zhang, F. Zhu, X. Zhuang, R. Jordan, O. G. Schmidt, and X. Feng, "Thermoswitchable on-chip microsupercapacitors: One potential self-protection solution for electronic devices," Energy Environ. Sci. **11**, 1717–1722 (2018).

[8] C. Gao, J. Huang, Y. Xiao, G. Zhang, C. Dai, Z. Li, Y. Zhao, L. Jiang, and L. Qu, "A seamlessly integrated device of micro-supercapacitor and wireless charging with ultrahigh energy density and capacitance," Nat. Commun. **12**(1), 2647 (2021).

[9] K.-H. Lee, S.-S. Lee, D. B. Ahn, J. Lee, D. Byun, and S.-Y. Lee, "Ultrahigh areal number density solid-state on-chip microsupercapacitors via electrohydrodynamic jet printing," Sci. Adv. **6**(10), eaaz1692 (2020).

[10] X. Tang, H. Zhou, Z. Cai, D. Cheng, P. He, P. Xie, D. Zhang, and T. Fan, "Generalized 3D printing of graphene-based mixed-dimensional hybrid aerogels," ACS Nano **12**(4), 3502–3511 (2018).

[11] S. Sahoo, G. Sahoo, S. M. Jeong, and C. S. Rout, "A review on supercapacitors based on plasma enhanced chemical vapor deposited vertical graphene arrays," J. Energy Storage **53**, 105212 (2022).

[12] A. P. S. Gaur, W. Xiang, A. Nepal, J. P. Wright, P. Chen, T. Nagaraja, S. Sigdel, B. LaCroix, C. M. Sorensen, and S. R. Das, "Graphene aerosol gel ink for printing micro-supercapacitors," ACS Appl. Energy Mater. **4**(8), 7632–7641 (2021).

[13] Z.-S. Wu, K. Parvez, X. Feng, and K. Müllen, "Photolithographic fabrication of high-performance all-solid-state graphene-based planar micro-supercapacitors with different interdigital fingers," J. Mater. Chem. A **2**(22), 8288–8293 (2014).

[14] K. Li, X. Wang, S. Li, P. Urbankowski, J. Li, Y. Xu, and Y. Gogotsi, "An ultrafast conducting polymer@MXene positive electrode with high volumetric capacitance for advanced asymmetric supercapacitors," Small **16**(4), 1906851 (2020).

[15] K. Li, J. Zhao, A. Zhussupbekova, C. E. Shuck, L. Hughes, Y. Dong, S. Barwich, S. Vaesen, I. V. Shvets, M. Möbius *et al.*, "4D printing of MXene hydrogels for high-efficiency pseudocapacitive energy storage," Nat. Commun. **13**(1), 6884 (2022).

[16] G. Zhou, M. Li, C. Liu, Q. Wu, and C. Mei, "3D printed $Ti_3C_2T_x$ MXene/cellulose nanofiber architectures for solid-state supercapacitors: Ink rheology, 3D printability, and electrochemical performance," Adv. Funct. Mater. **32**(14), 2109593 (2022).

[17] S. Sollami Delekta, K. H. Adolfsson, N. Benyahia Erdal, M. Hakkarainen, M. Östling, and J. Li, "Fully inkjet printed ultrathin microsupercapacitors based on graphene electrodes and a nano-graphene oxide electrolyte," Nanoscale **11**(21), 10172–10177 (2019).

[18] Y. Bräuniger, S. Lochmann, J. Grothe, M. Hantusch, and S. Kaskel, "Piezoelectric inkjet printing of nanoporous carbons for micro-supercapacitor devices," ACS Appl. Energy Mater. **4**(2), 1560–1567 (2021).

[19] S. Sollami Delekta, M. Ostling, and J. Li, "Wet transfer of inkjet printed graphene for microsupercapacitors on arbitrary substrates," ACS Appl. Energy Mater. **2**(1), 158–163 (2018).

[20] J. Li, S. Sollami Delekta, P. Zhang, S. Yang, M. R. Lohe, X. Zhuang, X. Feng, and M. Östling, "Scalable fabrication and integration of graphene microsupercapacitors through full inkjet printing," ACS Nano **11**(8), 8249–8256 (2017).

[21] L. Li, E. B. Secor, K. Chen, J. Zhu, X. Liu, T. Z. Gao, J. T. Seo, Y. Zhao, and M. C. Hersam, "High-performance solid-state supercapacitors and microsupercapacitors derived from printable graphene inks," Adv. Energy Mater. **6**(20), 1600909 (2016).

[22] A. Nepal, G. P. Singh, B. N. Flanders, and C. M. Sorensen, "One-step synthesis of graphene via catalyst-free gas-phase hydrocarbon detonation," Nanotechnology **24**(24), 245602 (2013).

[23] J. P. Wright, S. Sigdel, S. Corkill, J. Covarrubias, L. LeBan, A. Nepal, J. Li, R. Divigalpitiya, S. H. Bossmann, and C. M. Sorensen, "Synthesis of turbostratic nanoscale graphene via chamber detonation of oxygen/acetylene mixtures," Nano Sel. **3**(6), 1054–1068 (2022).

[24] D. W. Kim, S. M. Jung, and H. Y. Jung, "A super-thermostable, flexible supercapacitor for ultralight and high performance devices," J. Mater. Chem. A **8**(2), 532–542 (2020).

[25] Y. Shao, J. Li, Y. Li, H. Wang, Q. Zhang, and R. B. Kaner, "Flexible quasi-solid-state planar micro-supercapacitor based on cellular graphene films," Mater. Horiz. **4**(6), 1145–1150 (2017).

[26] J. Gao, X. Wang, Y. Zhang, J. Liu, Q. Lu, and M. Liu, "Boron-doped ordered mesoporous carbons for the application of supercapacitors," Electrochim. Acta **207**, 266–274 (2016).

[27] S. Sahoo, P. Pazhamalai, V. K. Mariappan, G. K. Veerasubramani, N.-J. Kim, and S.-J. Kim, "Hydrothermally synthesized chalcopyrite platelets as an electrode material for symmetric supercapacitors," Inorg. Chem. Front. **7**(7), 1492–1502 (2020).

[28] P. K. Jha, S. K. Singh, V. Kumar, S. Rana, S. Kurungot, and N. Ballav, "High-level supercapacitive performance of chemically reduced graphene oxide," Chem **3**(5), 846–860 (2017).

[29] S. Wang, B. Hsia, C. Carraro, and R. Maboudian, "High-performance all solid-state micro-supercapacitor based on patterned photoresist-derived porous carbon electrodes and an ionogel electrolyte," J. Mater. Chem. A **2**(21), 7997–8002 (2014).

[30] F. Wen, C. Hao, J. Xiang, L. Wang, H. Hou, Z. Su, W. Hu, and Z. Liu, "Enhanced laser scribed flexible graphene-based micro-supercapacitor performance with reduction of carbon nanotubes diameter," Carbon **75**, 236–243 (2014).

[31] Y. Zhang, Y. Song, Y. Shi, Y. Wang, X. Wang, X. Shi, C. Tang, J. Liu, G. Wang, Q. Tan, and L. Li, "High-performance all-solid-state microsupercapacitors from 3D printing structure-engineered graphene-carbon sphere electrodes," Appl. Surf. Sci. **597**, 153730 (2022).

[32] L. Zhang, L. Liu, C. Liu, X. Li, F. Liu, W. Zhao, S. Wang, F. Wu, and G. Zhang, "Photolithographic fabrication of graphene-based all-solid-state planar on-chip microsupercapacitors with ultrahigh power characteristics," J. Appl. Phys. **126**(16), 164308 (2019).

[33] A. Khodabandehlo, A. Noori, M. S. Rahmanifar, M. F. El-Kady, R. B. Kaner, and M. F. Mousavi, "Laser-scribed graphene–polyaniline microsupercapacitor for the internet-of-things applications," Adv. Funct. Mater. **32**, 2204555 (2022).

[34] Y. Wu, Y. Zhang, Y. Liu, P. Cui, S. Chen, Z. Zhang, J. Fu, and E. Xie, "Boosting the electrochemical performance of graphene-based on-chip micro-supercapacitors by regulating the functional groups," ACS Appl. Mater. Interfaces **12**(38), 42933–42941 (2020).

[35] B. Liu, Q. Zhang, L. Zhang, C. Xu, Z. Pan, Q. Zhou, W. Zhou, J. Wang, L. Gu, and H. Liu, "Electrochemically exfoliated chlorine-doped graphene for flexible all-solid-state micro-supercapacitors with high volumetric energy density," Adv. Mater. **34**(19), 2106309 (2022).

[36] Y. Xie, J. Zhang, H. Xu, and T. Zhou, "Laser-assisted mask-free patterning strategy for high-performance hybrid micro-supercapacitors with 3D current collectors," Chem. Eng. J. **437**, 135493 (2022).

[37] J. Yang, Z. Pan, J. Zhong, S. Li, J. Wang, and P.-Y. Chen, "Electrostatic self-assembly of heterostructured black phosphorus–MXene nanocomposites for flexible microsupercapacitors with high rate performance," Energy Storage Mater. **36**, 257–264 (2021).

[38] A. Chaichi, G. Venugopalan, R. Devireddy, C. Arges, and M. R. Gartia, "A solid-state and flexible supercapacitor that operates across a wide temperature range," ACS Appl. Energy Mater. **3**(6), 5693–5704 (2020).

[39] S. Sahoo, K. Krishnamoorthy, P. Pazhamalai, V. K. Mariappan, and S.-J. Kim, "Copper molybdenum sulfide nanoparticles embedded on graphene sheets as advanced electrodes for wide temperature-tolerant supercapacitors," Inorg. Chem. Front. **6**(7), 1775–1784 (2019).

[40]K. Hung, C. Masarapu, T. Ko, and B. Wei, "Wide-temperature range operation supercapacitors from nanostructured activated carbon fabric," J. Power Sources **193**(2), 944–949 (2009).
[41]J. J. Yoo, K. Balakrishnan, J. Huang, V. Meunier, B. G. Sumpter, A. Srivastava, M. Conway, A. L. Mohana Reddy, J. Yu, R. Vajtai, and P. M. Ajayan, "Ultrathin planar graphene supercapacitors," Nano Lett. **11**(4), 1423–1427 (2011).
[42]L. Li, Z. Lou, W. Han, and G. Shen, "Flexible in-plane microsupercapacitors with electrospun $NiFe_2O_4$ nanofibers for portable sensing applications," Nanoscale **8**(32), 14986–14991 (2016).
[43]V. M. Maphiri, D. T. Bakhoum, S. Sarr, N. F. Sylla, G. Rutavi, and N. Manyala, "Impact of thermally reducing temperature on graphene oxide thin films and microsupercapacitor performance," Nanomaterials **12**(13), 2211 (2022).
[44]L. Wei, N. Nitta, and G. Yushin, "Lithographically patterned thin activated carbon films as a new technology platform for on-chip devices," ACS Nano **7**(8), 6498–6506 (2013).
[45]V. Sallaz, S. Oukassi, F. Voiron, R. Salot, and D. Berardan, "Assessing the potential of LiPON-based electrical double layer microsupercapacitors for on-chip power storage," J. Power Sources **451**, 227786 (2020).
[46]N. Kurra, B. Ahmed, Y. Gogotsi, and H. N. Alshareef, "MXene-on-paper coplanar microsupercapacitors," Adv. Energy Mater. **6**(24), 1601372 (2016).